J Solid State Electrochem (2010) 14:1241–1246
DOI 10.1007/s10008-009-0933-z

ORIGINAL PAPER

Preparation and electrochemical performance of monodisperse $Li_4Ti_5O_{12}$ hollow spheres

Ningde He · Binshuai Wang · Junjie Huang

Received: 17 June 2009 / Revised: 8 August 2009 / Accepted: 19 August 2009 / Published online: 16 September 2009

Abstract Monodisperse $Li_4Ti_5O_{12}$ hollow spheres were prepared by using carbon spheres as templates. Scanning electron microscopy images show hollow spheres that have an average outer diameter of 1.0 μm and an average wall thickness of 60 nm. Compared with $Li_4Ti_5O_{12}$ solids, the hollow spherical $Li_4Ti_5O_{12}$ exhibit an excellent rate capability and capacity retention and can be charged/discharged at 10 C (1.7 A g^{-1}) with a specific capacity of 100 mA h g^{-1}, and after 200 charge and discharge cycles at 2 C, their specific capacity remain very stable at 150 mA h g^{-1}. It is believed that the hollow structure has a relatively large contact surface between $Li_4Ti_5O_{12}$ and liquid electrolyte, resulting in a better electrochemical performance at high charge/discharge rate.

Keywords Lithium titanium oxide · Hollow spheres · Lithium ion battery · Carbon

Abbreviations

FTIR	Fourier transform infrared spectroscopy
XRD	X-ray diffraction
SEM	Scanning electron microscopy
LiAC	$LiCH_3COO$

Introduction

In lithium ion batteries, the rate determining step of the electrode reaction is the solid state diffusion of Li^+ ion in the active materials [1]. At high charge and discharge rates, high Li^+ ion insertion and exertion flux on the electrode surface and slow Li^+ ion transport result in concentration polarization of Li^+ ion within the electrode material. This phenomenon causes a drop of the cell voltage, which results in termination of the discharge before the maximum capacity of the electrode material is attained [2, 3]. In order to improve the rate capability of the electrode, materials with large surface areas and shorter Li^+ diffusion distances should be used in high rate lithium batteries.

Monodisperse hollow spheres with a controlled diameter and chemical composition have received rapidly growing interest because of its potential applications in delivery and controlled release systems, chromatography, adsorption, microreactors, and energy storage and conversion [4–6]. Due to their characteristic features, such as large surface areas and open pores, materials with hollow spherical particles have attracted more and more attention in high power batteries, in which rapid charge and discharge are required. As for the fabrication of hollow spheres, the most common approach is the template method. Suitable templates can be: silica [7], polymer [8–10], but also vesicles [11–13], emulsions [14–16], micelles (soft templates) [17, 18], and even gas bubbles [19]. In the template method, a layer of the desired chemical matter is coated or deposited on the surface of the spherical template, followed by removal of the spherical particles to leave behind a hollow structure.

$Li_4Ti_5O_{12}$ has attracted much interest due to its potential application as anode material in high rate lithium batteries. Compared with graphite-based anode materials, $Li_4Ti_5O_{12}$ shows many special characteristics [20, 21]: small volume change during charge/discharge process, which makes a stable electrode structure, benefiting for a long cycling life; a stable charge/discharge plateau at the potential of 1.55 V

N. He · B. Wang · J. Huang (✉)
College of Chemistry & Chemical Engineering,
Shaoxing University,
Shaoxing 312000, People's Republic of China
e-mail: hjj@zscas.edu.cn

(vs Li^+/Li), which can avoid the reduction of organic electrolyte and the deposition of metallic lithium, thus making batteries more safe. Furthermore, $Li_4Ti_5O_{12}$ is known as a good lithium ion conductor [22]. The combination of high lithium mobility and small volume change makes it an attractive anode for application in high rate batteries, but its low electron conductivity greatly influences its discharge ability at high rate.

The present work aims to improve the charge/discharge performance at high rate by using monodisperse $Li_4Ti_5O_{12}$ hollow spheres as anodic material. These hollow spheres were fabricated with carbon sphere templates, which were prepared through a hydrothermal route with glucose as a raw material. Usually, polymer spheres have been the most used templates for the preparation of hollow spherical electrode materials, but polymer spheres soften on heating, which leads to their distortion and coalescence, resulting in a structural collapse of the electrode materials. In contrast, during sintering carbon spheres are stable enough to form a uniform hollow structure of electrode materials. Unlike silicon template, carbon sphere templates can be easily removed, and their surface modification are unnecessary because their surfaces are full of hydrophilic group of –OH and $–COO^-$ with similarity to polysaccharide. During the preparation process of $Li_4Ti_5O_{12}$, lithium salt and Ti $(OC_4H_9)_4$ can be adsorbed into the template surface layer due to the strong bonding ability of –OH and $–COO^-$ groups. After removal of the template in air at high temperature, $Li_4Ti_5O_{12}$ hollow spheres were formed. Since the thickness of the functional "surface layer" is predetermined by hydrothermal synthesis, the integrity and uniformity of the shell of final products can be ensured in this way. Using carbon spheres as template, $Li_4Ti_5O_{12}$ hollow spheres with different wall thickness have been prepared through controlling the loading amount of template by C. Jiang [23], but the monodisperse $Li_4Ti_5O_{12}$ hollow spheres have not been obtained. In the present study, monodisperse $Li_4Ti_5O_{12}$ hollow spheres are fabricated through a new preparation route with carbon spheres as template, and their electrochemical characteristics were investigated.

Experimental section

The preparation of carbon template spheres: In a typical procedure, sucrose (4 g, analytic purity, Beijing Chemical Reagent Factory) was dissolved in distilled water (35 ml) to form a clear solution. The solution was then sealed in a 40 ml teflon-lined autoclave and maintained at 170 °C for 10 h. The black or puce products were isolated after centrifugation at 5,000 rpm for 20 min. The products were centrifuged, washed, and redispersed in water, and this cycle was repeated five times. Next, the products were centrifuged, washed, and redispersed in alcohol, and this cycle was repeated five times. The spheres were then oven-dried at 80 °C for 4–8 h.

The preparation of $Li_4Ti_5O_{12}$ hollow spheres: Firstly, a suspension was obtained by dispersing carbon spheres (100 mg) in 15 ml $LiCH_3COO$ (LiAC) ethanol solution (containing 195 mg $LiCH_3COO{\cdot}2H_2O$) using ultrasonic dispenser; then, $Ti(OC_4H_9)_4$ (735 mg) was dropped into it and kept stirring for 1 h. After that, the solvent was vaporized at 70 °C on an oil bath with constant slow stirring. The obtained black powder was the precursor of $Li_4Ti_5O_{12}$ containing carbon spheres' template. Finally, the precursor was first calcinated in air at 450 °C for 5 h with a ramp of 2 °C/min from room temperature to 450 °C, and then the temperature was increased to 800 °C with a heating ramp of 5 °C/min and maintained at 800 °C for 10 h. After cooling down, the $Li_4Ti_5O_{12}$ hollow spheres (LTO-1) were prepared.

For comparison, solid particles of $Li_4Ti_5O_{12}$ were prepared as reported in literature [24], Briefly, $Ti(OC_4H_9)_4$ was mixed with *n*-heptane in a ratio of 1:10 (weight ratio), and $LiAC{\cdot}2H_2O$ was dissolved in 90% ethanol in the ratio of 1:20 (weight ratio), respectively. Then, the LiAC ethanol solution was added dropwise slowly into $Ti(OC_4H_9)_4$ *n*-heptane solution (at the molar ratio of Li:Ti=4.4:5) under magnetic stirring. During the addition, a white sol–gel appeared as a result of $Ti(OC_4H_9)_4$ hydrolysis. After 1 h stirring, the white sol–gel solution was heated at 65 °C for removal of the solvent and final isolation of the precursor. Then, the precursor was heated at 450 °C in N_2 atmosphere for 5 h and further calcinated at 800 °C for another 10 h. Finally, a white powder of spinel $Li_4Ti_5O_{12}$ (LTO-2) was obtained.

The surface functional groups of the carbon sphere template were characterized by Fourier transform infrared spectroscopy (FTIR; Nexus 670, America Nicolet Co.). X-ray diffraction (XRD) were recorded on a Bruker D8 advanced diffractometer with Cu Kα radiation. The morphology of $Li_4Ti_5O_{12}$ hollow spheres was characterized by scanning electron microscopy (SEM) (Philips XL 30).

Cyclic voltammetries of $Li_4Ti_5O_{12}$ electrodes were carried out using a CHI660 electrochemical workstation (CHI USA) in a conventional three-electrode cell; two lithium plates were used as the reference and the counter electrode, respectively. The charge–discharge performance and the cycling stability of $Li_4Ti_5O_{12}$ electrodes were tested by the electrochemical equipment of Land (Wuhan Land electrochemical equipment company, China). The cell consisted of a working electrode (active material:carbon black:polytetrafluoroethylene binder=80:15:5 wt%), a metal lithium foil electrode, and a Celgard 2300 separator. The electrolyte was 1 mol/L $LiPF_6$ in the mixture of ethylene carbonate and dimethyl carbonate (1:1 *v*/*v*%; Ferro Com.). The cells were assembled in a dry glove box. The charge–discharge cycling

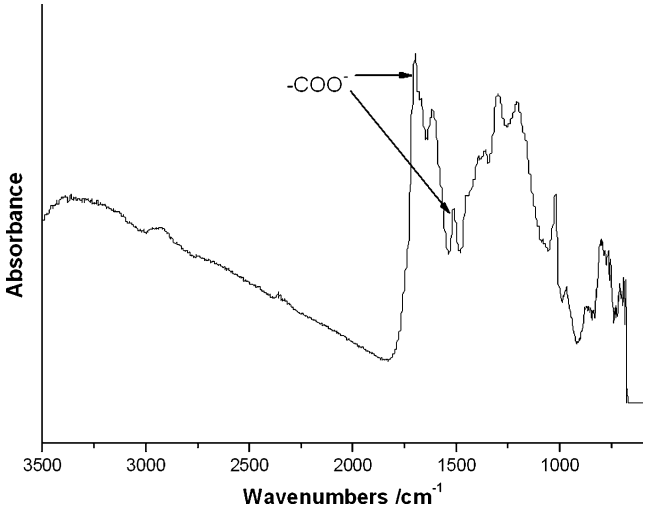

Fig. 1 FTIR spectrum of carbon sphere template

test was carried out galvanostatically at different values of current density. The cut-off voltages for charge and discharge processes were 3 and 1 V, respectively. Experiments were carried out at room temperature.

Results and discussion

FTIR spectroscopy was used to identify the functional groups after hydrothermal treatment. The bands at 1,699 and 1,512 cm^{-1} (Fig. 1) indicated that the surface of carbon spheres contained COO^- group. The bands in the range of 1,000–1,300 cm^{-1} were attributed to C–OH stretching and OH bending vibrations and were related to –OH groups on the template surface. The presence of these groups favors the adsorption of Li^+ and $Ti(OC_4H_9)_4$ onto the template surface.

Figure 2a showed the SEM image of carbon templates. It can be clearly observed that the carbon spheres had a narrow size distribution with an average diameter of about 2.0 μm. Figure 2b showed the SEM morphology of LTO-1. Many hollow spheres constructed by nanoparticles (<100 nm) can be observed clearly, and the average diameter and wall thickness are about 1.0 μm and 60 nm, respectively. The diameters of $Li_4Ti_5O_{12}$ hollow spheres are about 50% smaller than that of carbon spheres. The large shrinkage ratio essentially differs from one obtained using traditional sacrificial-core methods [8, 9]. In these methods, the prepared hollow spheres were nearly the same size or slightly smaller than their templates. The shrinkage was also found in the preparation of hollow spherical Ga_2O_3 and GaN using carbon spheres as template [25]. The possible explanation should be the further dehydration of the loosely cross-linked structure of the carbon spheres, which leads to the densification of $Li_4Ti_5O_{12}$ precursors in the surface layer of template. Their fabricating process was presented in Fig. 2c and can be explained as follows: due to the strong bonding ability of –OH and –COO groups, $LiCH_3COO$ and $Ti(OC_4H_9)_4$ can be adsorbed into carbon surface layer, with subsequent hydrolysis of adsorbed $Ti(OC_4H_9)_4$; the precursor of $Li_4Ti_5O_{12}$ deposits in the surface layer of carbon spheres. Consequently, crystallization of $Li_4Ti_5O_{12}$ takes place when the carbon is removed at air atmosphere during the calcinating process, thus resulting in $Li_4Ti_5O_{12}$ hollow

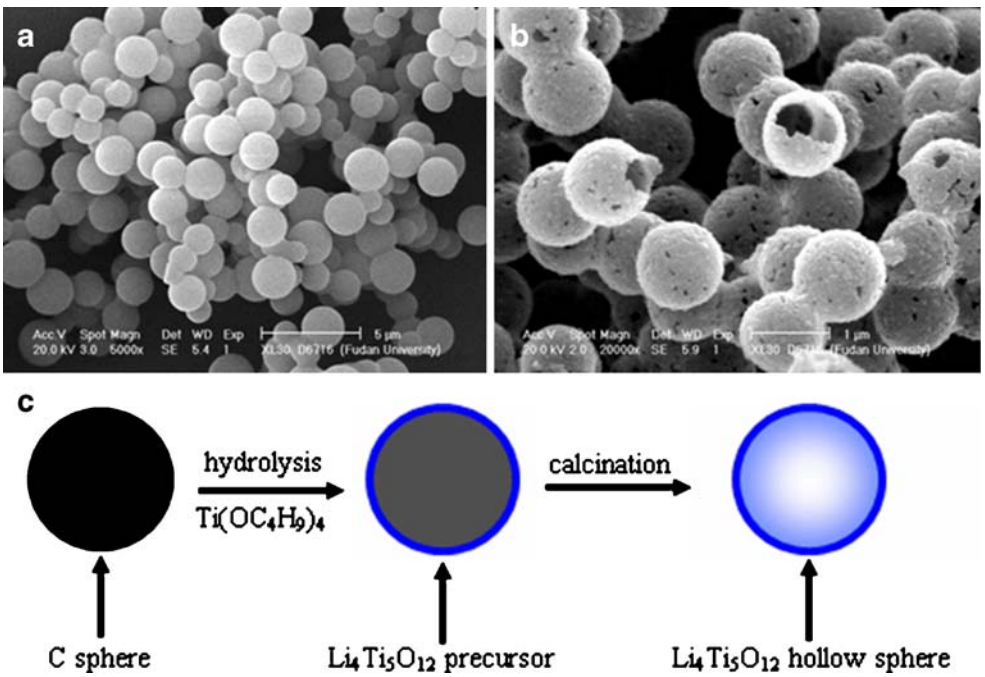

Fig. 2 SEM images of carbon spheres (**a**), $Li_4Ti_5O_{12}$ hollow spheres (**b**), and schematic mechanism for the formation of $Li_4Ti_5O_{12}$ hollow spheres(**c**)

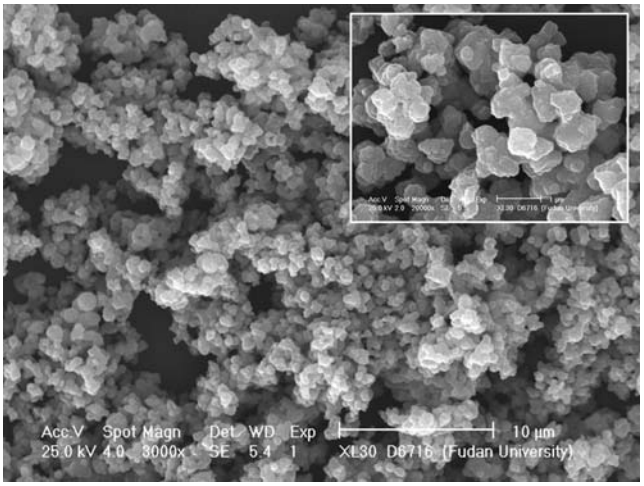

Fig. 3 SEM images of $Li_4Ti_5O_{12}$ solid particles (LTO-2)

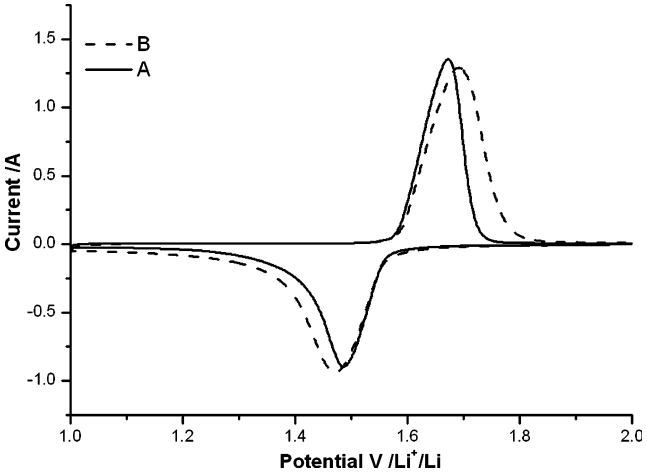

Fig. 5 Cyclic voltagrametric figures of $Li_4Ti_5O_{12}$ electrode: LTO-1 (*A*), LTO-2 (*B*)

spheres. Figure 3 shows the SEM image of LTO-2; solid particles are observed, and some of them aggregated together. From the high magnification image (the inner picture in Fig. 3), the sintered grains are closely packed by small particles with the size of about 100–500 nm.

Figure 4 illustrated XRD patterns of LTO-2 and LTO-1 samples, respectively. According to JCPDS file no. 26-1198, in both curves, the diffraction peaks located at the 2θ of 18.4°, 35.6°, 37.2°, 43.3°, 47.4°, 57.3°, 62.8°, and 66.1° can be indexed to the crystallographic planes of (111), (311), (222), (400), (331), (333), (440), and (531) of spinel $Li_4Ti_5O_{12}$, respectively. No peaks attributed to TiO_2 or other phases were found in XRD patterns. According to XRD results, both materials had a spinel crystal structure.

Figure 5 displayed the cyclic voltammetries of LTO-1 and LTO-2 electrodes between 1.0 and 2.0 V at the scan rate of 0.1 mV s^{-1}. The behaviors of cyclic voltammetry were taken by 10 cycles, and from the second cycle, the CV curves were no longer changeable. Therefore, all the curves used in the Fig. 5 were recorded in the fifth cycle. In both curve A and curve B, a couple of reversible redox peaks can be observed near the potential of 1.55 V vs Li^+/Li, which shows that Li^+ can successfully insert/extract into/from both materials. Compared with LTO-2 electrode, LTO-1 electrode has a more negative Li^+ extraction potential and a more positive Li^+ insertion potential. This should be due to the relative large contact surface area in hollow spheres between $Li_4Ti_5O_{12}$ and liquid electrolyte in favor of the insertion/extraction of Li^+.

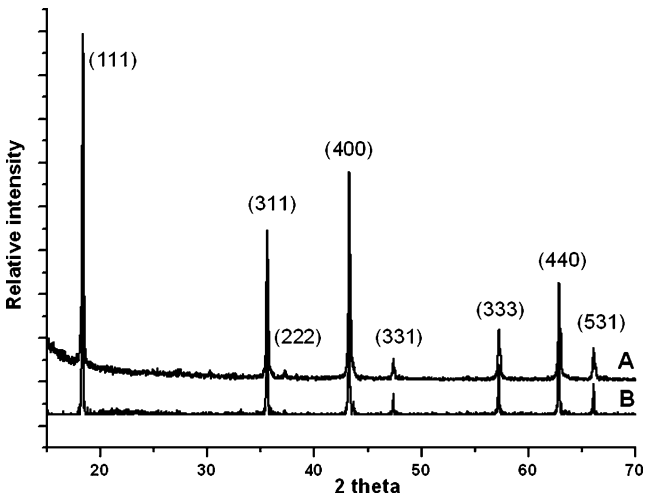

Fig. 4 XRD patterns of LTO-2(*A*) and LTO-1(*B*)

The charge–discharge curves of LTO-2 electrode at different current rates from 0.5 to 10 C were shown in Fig. 6b. In each rate, the charge/discharge process was taken by 10 cycles, and the used curve was recorded in the second cycle. As the charge–discharge rate increases, the capacity decreases quickly from 137 mA h g^{-1} (0.5 C) to 67 mA h g^{-1} (10 C). In constrast, the LTO-1 electrode has a great improvement on the rate capability, as shown in Fig. 6a. At the rates from 0.5 to 2 C, the variations of discharge plateau potential are very small, and the margin between charge and discharge plateau potentials is very small (about 40 mV). The discharge plateau potentials are near 1.55 V, which is the reversible redox potential of spinel $Li_4Ti_5O_{12}$, as suggested by S. Scharner et al. [26]. At the rate of 0.5 C, the discharge specific capacity is 165 mA h g^{-1}, which is very close to its theoretical capacity of 175 mA h g^{-1}. At the rate of 1, 2, 5, and 10 C, the discharge specific capacities are 158, 150, 122, and 100 mA h g^{-1}, respectively. This excellent rate capability is mainly due to its hollow structure, which allows the electrolyte to penetrate easily every $Li_4Ti_5O_{12}$ particles, making the insertion/extraction of Li^+ easy between liquid electrolyte and $Li_4Ti_5O_{12}$ particles. Furthermore, as shown in literature [23], hollow structured materials have more

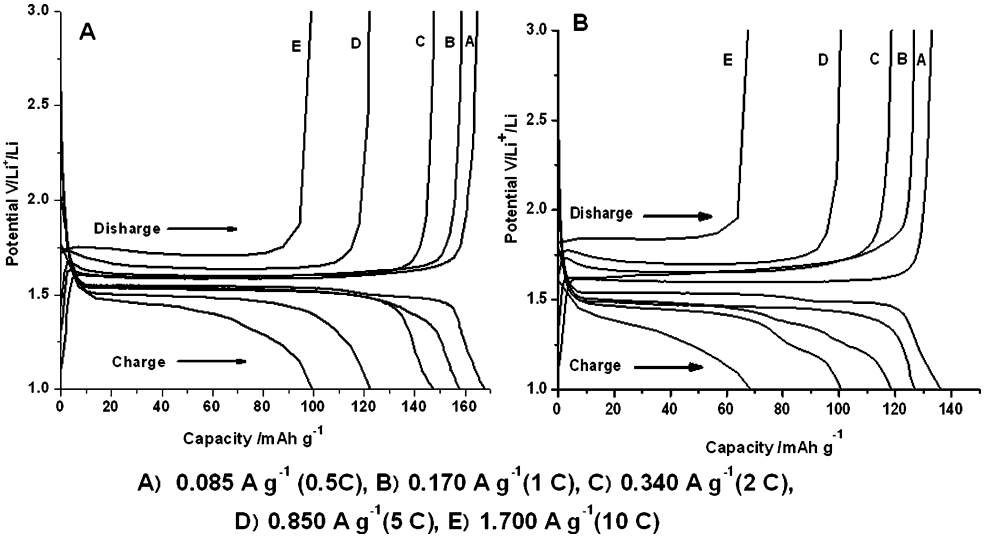

Fig. 6 Charge/discharge performance of electrode of LTO-1(**a**) and LTO-2(**b**) at different rates

$Li_4Ti_5O_{12}$ particles contact with conductive carbon in comparison with densely parked $Li_4Ti_5O_{12}$ grains, hence, improving the electronic conductivity. This may also help to improve the high rate performance.

In order to evaluate the cycling performance of LTO-1 electrode, the cell was progressively charged and discharged in a series stages with the charge/discharge rate from 0.5 to 10 C. For each stage, the process was taken by 10 cycles. Figure 7 showed the variation of discharge capacity in this experiment. In each stage, the discharge capacity kept very stable even at the rate of 10 C. After such 50 charge–discharge cycles, the $Li_4Ti_5O_{12}$ electrode was further charged and discharged at 2 C for another 200 cycles. The results are shown in Fig. 8. The discharge capacity is very stable. The discharge capacity in first cycle was 150 mA h g^{-1}, and after 200 charge–discharge cycles, the capacity also remained as 149.8 mA h g^{-1}. Figure 8 also shows that the charge and discharge efficiency in this long cycle period almost kept constant at 100%. The results show that the prepared $Li_4Ti_5O_{12}$ electrode has good capacity retention. The good rate capability and capacity retention can be attributed to the stable hollow structure.

Conclusions

In summary, $Li_4Ti_5O_{12}$ hollow spheres prepared by using carbon spheres as template showed an excellent charge/discharge performance over densely aggregated particles, which was mainly due to its stable hollow structure. Accordingly, both the large contact surface area between the $Li_4Ti_5O_{12}$ particle and electrolyte and the well mixing with conductive carbon improve the high rate performance.

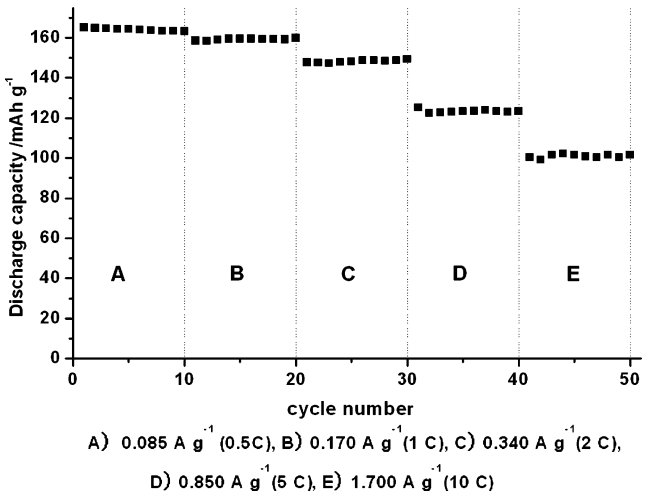

Fig. 7 Cycling response of LTO-1 electrode at various discharge rate at room temperature

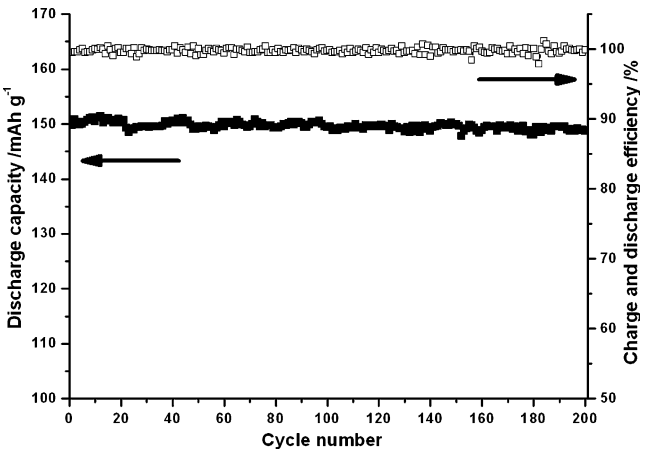

Fig. 8 Cycling performance and charge–discharge efficiency of LTO-1 electrode at the rate of 2 C

Acknowledgments This work was supported by the program of Shaoxing University (08LG1006).

References

1. Yin Y, Lu Y, Gates B, Xia Y (2001) Chem Mater 13:1146–1148
2. Strohm H, Sgraja M, Bertling J, Lobmann P (2003) J Mater Sci 38:1605–1609
3. Wang D, Caruso RA, Caruso F (2001) Chem Mater 13:364–371
4. Strohm H, Lobmann P (2004) J Mater Chem 14:2667–2673
5. Wang D, Caruso F (2002) Chem Mater 14:1909–1913
6. Su F, Zhao XS, Wang Y, Wang L, Lee J (2006) J Mater Chem 16:4413–4419
7. Salgueirino-Maceira V, Spasova M, Farle M (2005) Adv Funct Mater 15(6):1036–1040
8. Caruso F, Spasova M, Saigueirino-Maceira V, Liz-Marzan LM (2001) Adv Mater 13(14):1090–1094
9. Shiho H, Kawahashi N (2000) Colloid Polym Sci 278(3):270–274
10. Kawahashi N, Persson C, Matijevic E (1991) J Mater Chem 1 (4):577–582
11. Schmidt HT, Ostafin AE (2002) Adv Mater 14(7):532–535
12. Hubert DHW, Jung M, German AL (2000) Adv Mater 12 (17):1291–1294
13. Hentze HP, Raghavan SR, McKelvey CA, Kaler EW (2003) Langmuir 19(4):1069–1074
14. Hirai T, Hariguchi S, Komasawa I, Davey RJ (1997) Langmuir 13 (25):6650–6653
15. Wu MM, Wang GG, Xu HF, Long JB, Shek FLY, Lo SMF, Williams ID, Feng SH, Xu RR (2003) Langmuir 19(4):1362–1367
16. Fowler CE, Khushalani D, Mann S (2001) Chem Commun 19:2028–2029
17. Fowler CE, Khushalani D, Mann S (2001) J Mater Chem 11 (8):1968–1971
18. Huang JX, Xie Y, Li B, Liu Y, Qian YT, Zhang SY (2000) Adv Mater 12(11):808–811
19. Du FL, Guo ZY, Li GC (2005) Mater Lett 59(19–20):2563–2565
20. Arico AS, Bruce P, Scrosati B, Tarascon JM, Schalkwijk WV (2005) Nat Mater 4:366–377
21. Du N, Zhang H, Chen BD, Wu JB, Ma XY, Liu ZH, Zhang YQ, Yang DR, Huang XH, Tu JP (2007) Adv Mater 19:4505–4509
22. Takai S, Kamata M, Fujine S, Yoneda K, Kanda K, Esaka T (1999) Solid State Ionics 123:165–172
23. Jiang C, Zhou Y, Honma I, Kudo T, Zhou H (2007) J Power Sources 166:514–518
24. Huang J, Jiang Z (2008) Electrochim Acta 53:7756–7759
25. Sun X, Li Y (2004) Angew Chem Int Ed 43:3827–3831
26. Scharner S, Weppner W, Schmid-Beurmann P (1999) J Electrochem Soc 146:857–861